

Type of the Paper (Abstract, Meeting Report, Preface, Proceedings, etc.)

Docking studies of 1,5-disubstituted tetrazoles analogs of the anticancer drug imatinib as probable inhibitors of the ABL kinase and the T315I mutant kinase[†]

Abel Suárez-Castro^{1*}, Carlos J. Cortes-García^{2*}, Rocío Gamez-Montaña³ and Luis Chacón-García^{1*}.

¹ Laboratorio de Diseño Molecular, Instituto de Investigaciones Químico Biológicas, Universidad Michoacana de San Nicolás de Hidalgo. Ciudad Universitaria, C.P. 58033, Morelia, Michoacán, México; lchacon@umich.mx

² Laboratorio de Investigación y Desarrollo, Apotex, API Toluca, Av. Industria Automotriz 301 Col. Zona Industrial Toluca, C.P. 50071, Toluca, Edo. Mex., México; quimcharly@gmail.com

³ Departamento de Química, División de Ciencias Naturales y Exactas, Universidad de Guanajuato, Noria Alta S/N, Col. Noria Alta, C.P. 36050, Guanajuato, Gto., México; rociogm@ugto.mx

* Correspondence: quimcharly@gmail.com; Tel.: +52(722)2757007 ext 199

† Presented at the title, place, and date.

Academic Editor: name

Received: date; Accepted: date; Published: date

Abstract: A docking studies of a set of several 1,5-disubstituted tetrazoles (1,5-DS-T) compounds to find potential inhibitors of the Abelson tyrosine-protein kinase (ABL kinase) and the mutated ABL kinase T315I were conducted by using Lamarckian genetic algorithms as search algorithms in Autodock4. Bayesian calculations were performed, and specificity (Sp) and sensitivity (Se) values as well as positive predicted values (PPVs) and negative predicted values (NPVs) were calculated using a set of 99 active ligands and 385 decoys for ABL kinase from the DUD database. RMSD values were calculated between the X-ray crystallographically determined coordinates of the ligands in the complexes of ligand with the ABL kinase and with T315I ABL kinase resistant to imatinib. The predicted results showed the importance of the interactions of the protein with halogens present in some of these 1,5-DS-T ligands. In conclusion, the results suggest that eight novel 1,5-DS-T compounds were identified to be effective inhibitors of ABL kinase.

Keywords: 1,5-DS-T, ABL kinase, Docking.

1. Introduction

Chronic myelogenous leukemia (CML) is a human disease characterized by a translocation between chromosomes 9 and 22 into the c-abl locus of chromosome 9 and the bcr region of chromosome 22 [1]. Its incidence is 2 per 100 000 each year and the common age of diagnosis of the disease is 50 to 55 [2]. ABL tyrosine kinases constitute a family of proteins with the best-conserved branches of the tyrosine kinases. There are two types of ABL tyrosine kinases: ABL1, which is involved in repairing damage to nuclear DNA, and ABL2, which binds actin and microtubules and is involved in cytoskeletal remodeling [3]. ABL genes have been observed in a tumor gene in the Abelson murine lymphosarcoma virus [4]. Patients with CML express a BCR-ABL1 oncoprotein that enhances the tyrosine kinase activity of the cells, leading to down-regulation of cell growth and of replication-associated pathways such as those that use JAK/STAT, MAPK, RAS, RAF, JUNK and MYC [5]. Treatments for CML have included allogenic stem cell transplantation and the use of recombinant interferon-alpha, but the most effective treatments have involved the administration of tyrosine kinase inhibitors (TKIs) [6] Imatinib mesylate was the first TKI drug found to function

against CML and to be well tolerated. Administration of this drug led to a complete cytogenetic response in 60 percent of cases and resulted in adverse events in less than 6 percent of patients, whereas the complete cytogenetic response rate for recombinant-interferon has been reported to be only 41% [7]. The chemical optimization of imatinib [8] is shown in Figure 1.

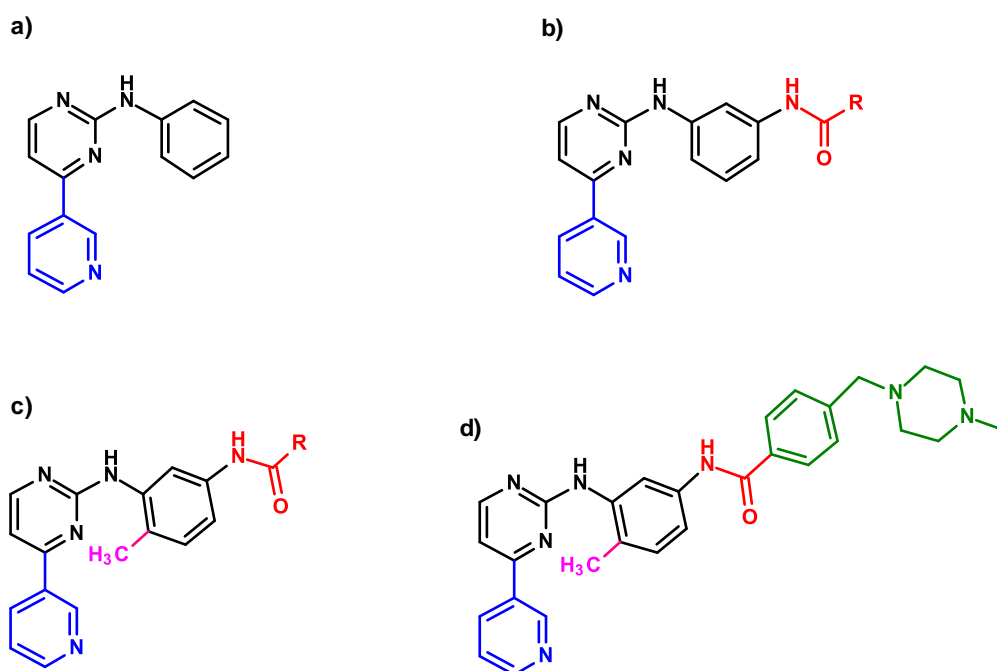


Figure 1. Schematic representation of the moieties in imatinib (d). The color code is provided in the text

Here, a phenylamino derivative is the core structure of the lead compound (and shown in black in the figure). The addition of a 3-pyridyl group (in blue in panels a-d) to the 3'-position of the pyrimidine enhanced the activity. The amide group (in red in panels b-d) conferred activity against tyrosine kinases. Addition of a methyl group (in pink in panels c and d) abolished the undesirable protein-kinase-C inhibitory activity. Finally, inclusion of *N*-methyl piperazine (in green in panel d) increased the solubility and oral bioavailability.

Type I, II and IV TKIs, including imatinib, nilotinib, dasatinib, bosutinib and ponatinib, have shown activity against Bcr-Abl and have been approved by the FDA (Figure 2), and about 36 compounds have been patented during the last 8 years [9]. Nevertheless, imatinib has been shown to lose its effectiveness against CML in up to 30% of patients during their first five years on therapy [10]. Here, various point mutations in the kinase domain of the Bcr-Abl protein (in particular between kinase domains) appear to cause such ineffectiveness of imatinib, by interfering with the interaction between the protein and the drug [10]. The mutations that most interfere with the drug activity are those at residues 255 and 315, with a mutation at residue 255 countering the inhibitory activity of nilotinib as well as of imatinib, and the T315I mutation (resulting in BCR-ABL T315I) interfering with the inhibitory activities of all TKIs [10].

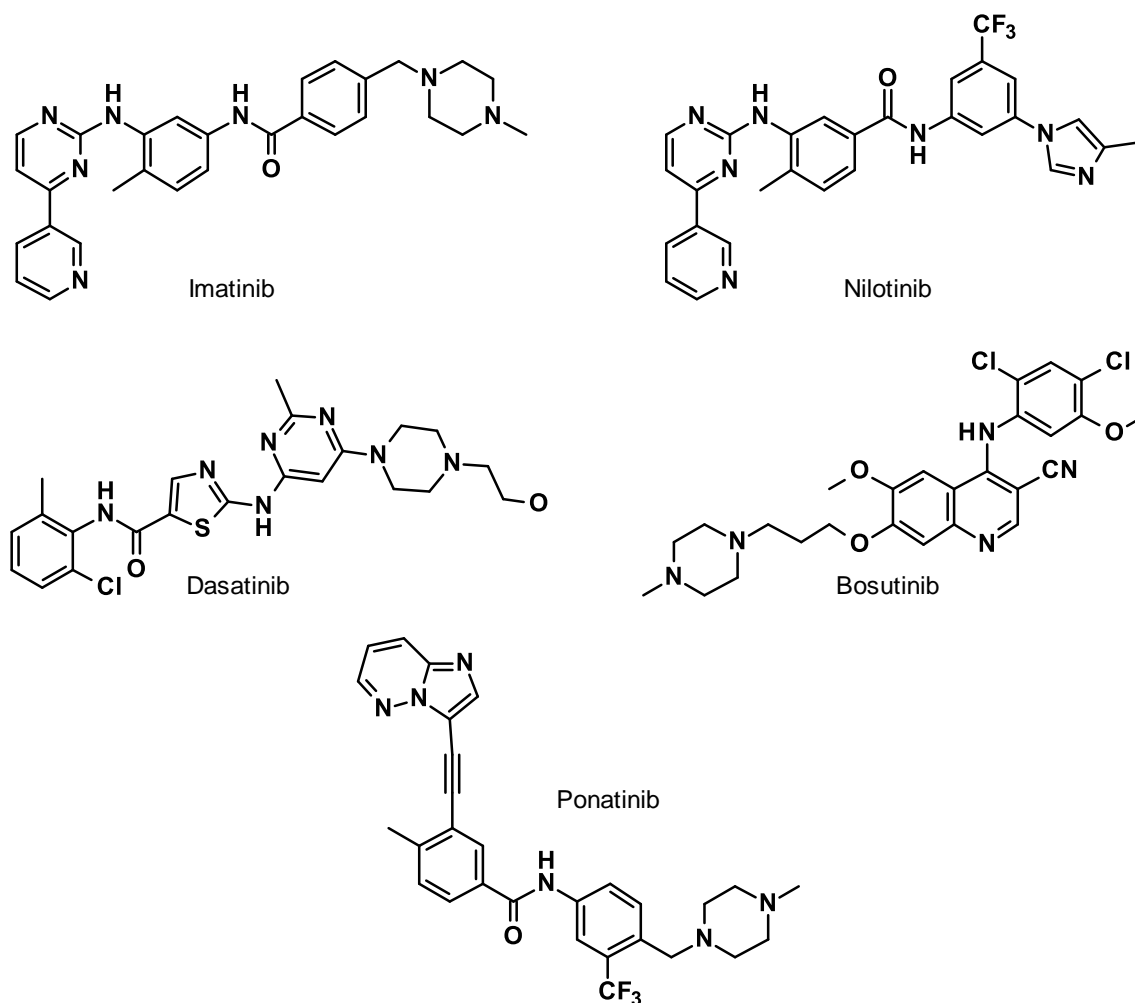


Figure 2. FDA approved drugs that inhibit the ABL kinase

Many efforts are being expended to find inhibitors of ABL kinase that remain active even toward resistant mutations in T315I. One good example is the compound PPY-A, which Zhou et al. [11] showed to have favorable interactions with and be a potential inhibitor of the T315I ABL kinase. The PDB code: 4TWP [12] was used for the docking studies with the novel 1,5-DS-T compounds as ligands in this study.

The resistance showed for the ABL kinase is a good reason to explore the behavior of new compounds with different scaffolds to find therapeutics that are effective against BCR-ABL T315I. Here, predicted interactions and affinity using molecular docking studies of novel 1,5-disubstituted-1H-tetrazoles synthesized via the Ugi-azide reaction by Carlos Cortés et al. are presented [13]. these novel compounds are used since they include a fragment of imatinib (Figure 3).

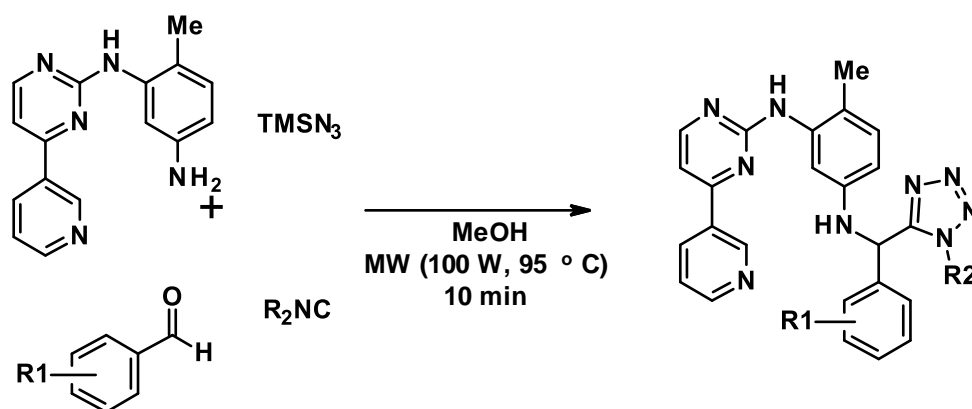


Figure 3. Overview of the synthesis of the new 1,5-DS-T compounds

2. Materials and methods

2.1 Compounds data set

To assess the docking protocol performance, the Bayesian theorem to 99 compounds known to be active against ABL kinase and 385 decoys for this kinase was applied. Both sets of compounds were retrieved from the Directory of Useful Decoys (DUD) [14] (www.dud.docking.org). Also, thirty-eight variants of 1,5-DS-T were synthesized by Cortés-García et al. and used as exploration set of compounds, these structures are listed in table 1. The ligands AXI and JIN as reference crystallographic structures that came from the PDB codes used in this research (4TWP and 2HZI respectively) to compare the RMSD values after the docking calculations have been used.

2.2 Computational experiments

The 1,5-DS-T compounds synthesized by Cortes-García et al. were modeled as 2D structures with the software ChemBio Draw Ultra 12.0 and converted into 3D structures in MDL format. Their protonated states were then calculated using Chemicalize [15] (www.chemicalize.org), and these structures were then retrieved in a .mol file for subsequent studies.

Table 1. Novel 1,5-DS-T compounds synthesized by Cortes-Garcia et al.

Entry	Compound code	R1	R2
1	1a	H	Cy
2	1b	H	<i>t</i> -Bu
3	2a	4-F	Cy
4	2b	4-F	<i>t</i> -Bu
5	3a	2-F	Cy
6	3b	2-F	<i>t</i> -Bu
7	4a	2,3-di-F	Cy
8	4b	2,3-di-F	<i>t</i> -Bu
9	5a	2,4-di-F	Cy
10	5b	2,4-di-F	<i>t</i> -Bu
11	6a	2,5-di-F	Cy
12	6b	2,5-di-F	<i>t</i> -Bu
13	7a	3,4-di-F	Cy
14	7b	3,4-di-F	<i>t</i> -Bu
15	8a	2,3,4,5,6-Penta-F	Cy
16	8b	2,3,4,5,6-Penta-F	<i>t</i> -Bu

17	9a	2-Cl	Cy
18	9c	2-Cl	<i>t-Bu</i>
19	10a	4-Cl	Cy
20	10b	4-Cl	<i>t-Bu</i>
21	11a	2-Br	Cy
22	11b	2-Br	<i>t-Bu</i>
23	12a	4-Br	Cy
24	12b	4-Br	<i>t-Bu</i>
25	13a	4-OMe	Cy
26	13b	4-OMe	<i>t-Bu</i>
27	14a	3,4-di-OMe	Cy
28	14b	3,4-di-OMe	<i>t-Bu</i>
29	15a	2,3,4-tri-OMe	Cy
30	15b	2,3,4-tri-OMe	<i>t-Bu</i>
31	16a	2,4,5-tri-OMe	Cy
32	16b	2,4,5-tri-OMe	<i>t-Bu</i>
33	17a	3,4,5-tri-OMe	Cy
34	17b	3,4,5-tri-OMe	<i>t-Bu</i>
35	18a	2,4,5-tri-Me	Cy
36	18b	2,4,5-tri-Me	<i>t-Bu</i>
37	19a	4-(pyridin-2-yl)	Cy
38	19b	4-(pyridin-2-yl)	<i>t-Bu</i>

The active and inactive structures from the DUD database were minimized by carrying out molecular mechanics using the UFF force field [16] in the Gaussian 3.9 software package [17] and the outputs were converted into .pdb files to prepare the ligands for the molecular docking studies.

2.3 Docking ligand preparation

Using Autodock Tools [18], one ligand was prepared to adding polar hydrogens and Gasteiger charges, rotatable (i.e., single) bonds were assigned by default, and a .pdbqt file was generated. This file was used as a template for the preparation of the rest of the ligands using the tool Raccon [19] that allows many structures to be prepared in .pdbqt file at the same time.

2.4 Docking receptor preparation

Two X-ray structures for the ABL kinase were downloaded in .pdb format from the PDB database [20]: PDB i.d. 2HZI, which contains the ligand JIN [21], and PDB i.d. 4TWP, which contains the ligand AXI [21]. The first one showed good interactions in the active site of ABL kinase and the second one for the T315I ABL kinase. After the preparation of the ligands in Autodock Tools, these X-ray structures were analyzed using Swiss PDB viewer [22] in order to find and correct any errors and to model any missing atoms, and after their minimized states were calculated using the AMBER force field in GROMACS adding polar hydrogens throughout the structures. Then, Kollman charges were added using Autodock Tools, and .pdbqt formats were generated for the docking calculations.

2.5 Docking experiments

Autodock4 was used for rigid docking calculations using the Lamarckian genetic algorithm [23]. Tetrazole ligands were set in a 126 Å x 126 Å x 126 Å grid box. A value of 0.37 was used for spacing calculations for the active and inactive ligands from the DUD database and these ligands were centered in each receptor. AD4.dat parameters were applied to all the ligands. Thus two different templates were generated, and formatted into .gpf and .dlg files, and then all of the ligands prepared for docking were obtained using the Raccon tool from Autodock Tools. The

conditions for the docking calculations were in general 100 runs, a population size of 150, a total of 1000000 generations, a default value of 0.8 for the crossover rate, a mutant rate of 0.2, and 100 individuals in each run [24].

2.6 Docking performance assessment

Scoring functions are commonly used to assess docking performance. In our study, decoys for ABL kinase, i.e., the compounds in the DUD database that are not active towards the kinase, were used to assess the docking performance of the active compounds, and then specificity and sensitivity values were obtained. The pKi values predicted from the negative and positive docking results were used as markers to distinguish active from inactive compounds [25]. Also, the original ligands from each receptor (JIN and AXI) were docked with the same conditions used for all other ligands in order to assess the performance of the docking using the RMSD value between the original coordinates and the predicted ones resulting from our docking protocol.

2.6 Docking results analysis

All of the results for each ligand were analyzed in Autodock Tools. The best free energies and Ki values were kept and afterwards the Ki values were converted in pKi values using equation 1. All of the information was processed in order to obtain the representative graphics comparing the free energy and pKi values.

The analysis of hydrogen bonds was carried out for the complexed ligands and the docked ones, each with their respective receptor, using HBAT software [26], in order to determine the principal and important interactions. PyMol software was used to visualize the interactions.

3. Results and discussion

3.1 Evaluation of the scoring function and search algorithm used in Autodock4.

For all of the 584 total of compounds tested in docking studies, predicted free energy and Ki values were obtained and compiled for statistical analysis. Each ligand was analyzed using the graphical interface of Autodock Tools to determine the pose and whether the ligand was bound in the active site. Two plots (for active compounds and decoys) were made to reveal the general behavior of the pKi and free energy (Figures 4 and 5).

$$pKi = -\log\left(\frac{Ki}{1 \times 10^6}\right) \quad \text{Equation 1}$$

3.2 Statistical results

The statistical results were obtained using the Bayesian theorem [27] with equations 2a, 2b, 2c, and the results are presented in table 2.

Table 2. Statistical results obtained using the Bayesian theorem

N = 584				
Active compounds = 99			Inactive compounds = 385	
True positives	False negatives	True negatives	False positives	Cutoff
85	14	123	262	10% (58)
Sensitivity (Se)			0.85	
Specificity (Sp)			0.31	
Enrichment Factor (EF)			10.79	
Positive Predicted Value (PPV)			0.24	
Negative Predicted Value (NPV)			1.12	
(LR)			1.26	

The positive predicted and negative predicted values are the probabilities of finding as positive or negative one event [28]. In this case, the results of the evaluation of the conditions in the docking protocol helped us determine how the genetic algorithm worked with the chemical environment of the receptor and the chemical structures of active and inactive ABL kinase compounds.

Bayesian equations

$$Se = \frac{TP}{TP+FN} \quad \text{equation 2a}$$

$$Sp = \frac{TN}{TN+FP} \quad \text{equation 2b}$$

$$PPV = \frac{TP}{TP+FP} \quad \text{equation 2c}$$

$$NPV = \frac{TN}{TN + FN} \quad \text{equation 2d}$$

Where: Se= Sensitivity; Sp= Specificity; TP= True positives; FN= False negatives; PPV= Positive predicted value; NPV= Negative predicted value

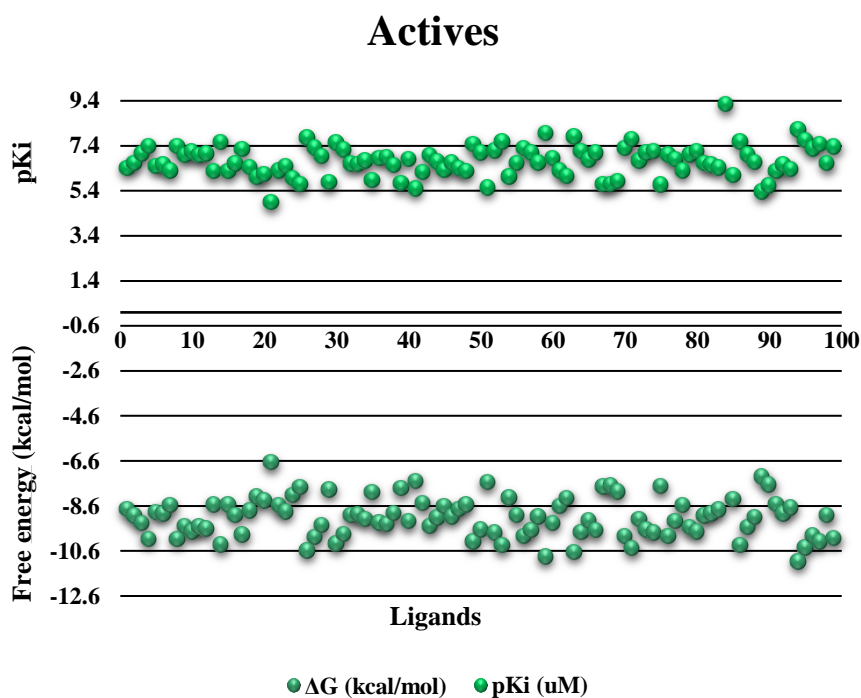


Figure 4. pKi and free energy values of the active set of ligands from the DUD database for the 2HZI receptor

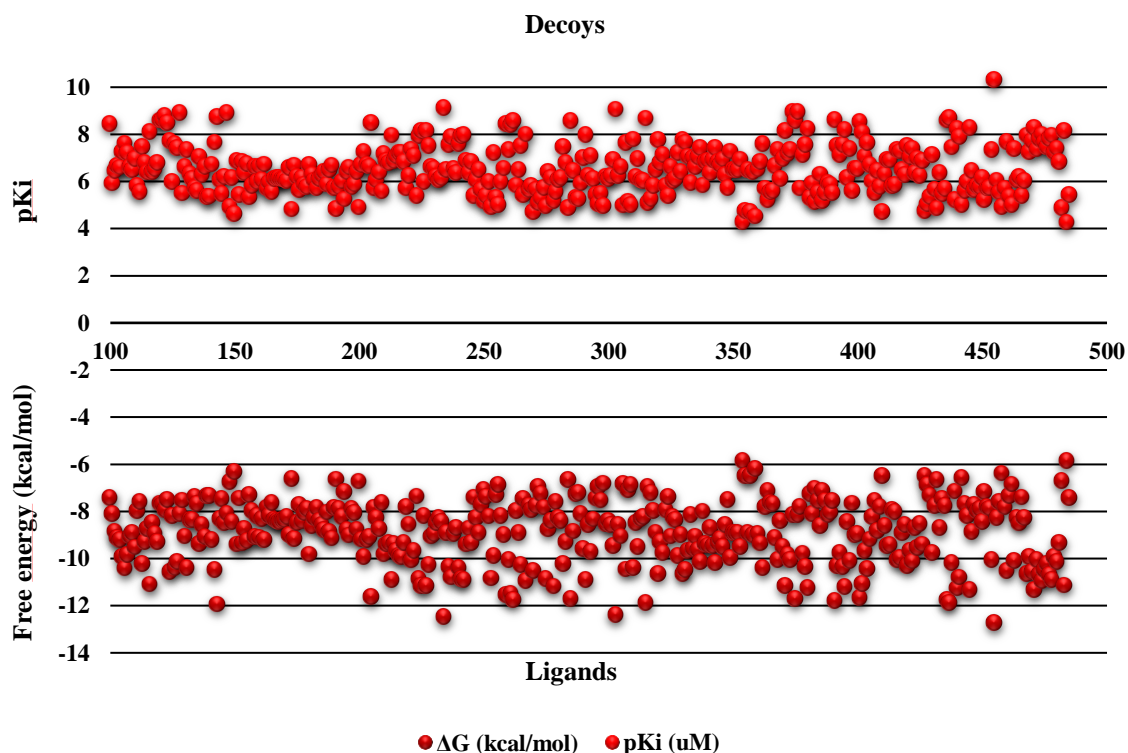


Figure 5 pKi and free energy values of the decoy (inactive) set of ligands from the DUD database for the 2HZI receptor

These results seem to be counterintuitive since decoys turn out to be false positives (262 compounds). The values used as cutoff to calculate the Se, Sp and for the PPV and NPV were using the pKi values from 6.03 – 9.24 (-8.2 to -12.6 kcal/mol) as actives (positive compounds), and below

pKi values from 6.02 (-8.18 Kcal/mol) as inactive (negative compounds) this based in the docking results of active compounds considered as active ones in de DUD data base. The results derived of the Bayesian calculations showed that there were more false positives than false negatives: Se = 0.85 and Sp = 0.31. It means that the protocol of the docking study could better predict positive ligands as the active compounds than it could predict the negative ligands as the inactive ones. Nevertheless, the PPV and the NPV showed us how the protocol has the possibility of detecting well the negative or inactive ligands; thus, the conditions of the docking experiment were considered for the docking validation calculations using the structural information for the 2HZI and 4TWP complexes as well the same conditions with the 38 novel 1,5-DS-T compounds.

3.3 Docking validation

The X-ray structures were prepared as is described in the general procedure for docking calculations, treating the ligands and receptors separately. The ligand in the 2HZI structure was identified as JIN and that in the 4TWP structure as AXI. After the calculations, the .dlg files were visualized using Autodock tools and the best free energy, affinity constant, and pose coordinate results were kept. Figure 6 shows a comparison of the original conformations of the ligands and those obtained from our calculations. The RMSDs were calculated using PyMol between the heavy atoms in the native and docked structures and were found to be 1.754 Å and 1.827 Å for the 2HZI_JIN and 4TWP_AXI complexes, respectively, were below 2.00 Å is the upper limit for validation of docking poses.

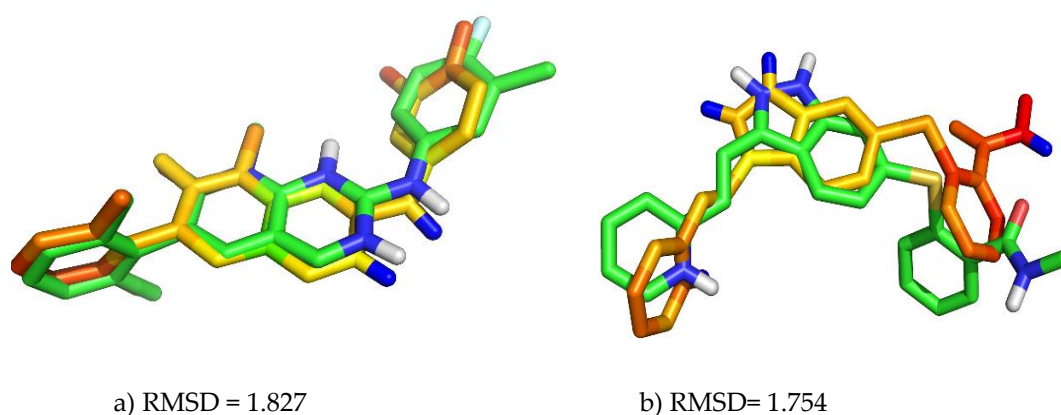


Figure 6 Superposition of complexed ligands and the predicted docking poses a: AXI from 4TWP, b: JIN from 2HZI

3.4 Evaluation of the novel 1,5-DS-T compounds with the docking protocol conditions.

The RMSD values resulting from the docking validation studies indicated that the conditions of the search method and the placement of coordinates in the grid box are appropriate for the 1,5-DS-T docking calculations. The 1,5-DS-T compounds were then prepared as were all of the ligands, and docking results of each compound were analyzed manually, and again the free energy, Ki values and the coordinates of the best pose were kept. The results are shown in the table 3.

The obtained results showed 3a, 9a, 11a and 11b to be the best ligands for the 2HZI receptor and 1a, 5a, 10a and 13a to be the best for the 4TWP receptor. The binding energies and the Ki values of the best ligands for the 2HZI receptor are very different from those for the 4TWP receptor. At the same time, it is important to remember that the 4TWP receptor is a mutated ABL kinase and these ligands, according to the docking results, could be tested in vitro to experimentally determine their activities against this protein.

Almost all the ligands interact with Lys 219 of the 2HZI protein and Met 316 of the 4TWP protein. To obtain all of the hydrogen bond interactions between the protein and the ligands, HBAT software was used to calculate the chemical properties of these bonds, and the results are shown in table 3. Lys 271 is the most common residue of the 2HZI receptor to which the ligands bind, while Met 316 is the most common residue of the 4TWP receptor to which the ligands bind. These interactions are shown in Figures 8 and 9. The results of the analysis of HBAT program using as starting structures the coordinates with the best-docked ligands are presented in table 4. Interestingly, the bests predicted affinities came from ligands that contain halogens, were those interactions involving halogens are well known in biological structures [29 - 33], suggesting that those interactions (except for fluorine which is not a halogen-bond donor) could correspond to the sigma hole halogen bonding. Unfortunately the scoring function used in our methodology, is not capable to predict accurately this kind of interactions. At the same time, comparing the structures of pairs of ligands as well as comparing their binding and K_i values revealed big differences between the results when the R2 moiety is cyclohexane and when it is a less hydrophobic group. Specifically comparing the ligands that have best interaction modes with their respective receptors led us to conclude that a more hydrophobic R2 moiety displays higher binding energies.

Table 3. Docking results of the 1,5-DS-T compounds with 2HZI and 4TP receptors.

Entry	Ligand	ΔG (kcal/mol)	K_i (nM)	pK_i (nM)	ΔG (kcal/mol)	K_i (nM)	pK_i (nM)
		2HZI			4TWP		
1	1a	-11.93	1.79	8.75	-12.89	1.79	9.45
2	1b	-11.28	5.4	8.27	-11.77	2.36	8.63
3	2a	-11.64	2.95	8.53	-13.04	2.95	9.56
4	2b	-10.98	8.88	8.05	-11.34	4.87	8.31
5	3a	-12.6	1.04	8.98	-12.58	1.04	9.22
6	3b	-11.36	0.101	8.33	-11.74	2.47	8.61
7	4a	-11.31	5.14	8.29	-12.23	1.09	8.96
8	4b	-10.99	8.86	8.05	-11.31	5.16	8.29
9	5a	-11.59	3.2	8.49	-12.82	3.2	9.4
10	5b	-11	8.61	8.06	-11.7	2.64	8.58
11	6a	-11.45	4.02	8.4	-11.57	3.32	8.48
12	6b	-11.14	6.8	8.17	-11.65	2.9	8.54
13	7a	-11.06	7.83	8.11	-12.16	1.22	8.91
14	7b	-10.95	9.45	8.02	-11.56	3.38	8.47
15	8a	-11.08	7.57	8.12	-11.76	2.41	8.62

16	8b	-10.89	10.45	7.98	-11.38	4.57	8.34
17	9a	-12.54	0.64	9.19	-11.49	3.81	8.42
18	9b	-11.8	2.25	8.65	-11.74	2.5	8.6
19	10a	-11.96	2.02	8.69	-13.73	2.02	10.06
20	10b	-11.34	4.84	8.32	-12.19	1.15	8.94
21	11a	-12.19	1.16	8.94	-12.22	1.1	8.96
22	11b	-12.39	0.82	9.08	-12.39	0.824	9.08
23	12a	-12.12	1.31	8.88	-13.24	1.31	9.71
24	12b	-11.44	4.1	8.39	-11.91	1.85	8.73
25	13a	-11.75	2.42	8.62	-13.8	2.42	10.11
26	13b	-11.07	7.65	8.12	-11.71	2.63	8.58
27	14a	-12.18	1.18	8.93	-12.26	1.04	8.98
28	14b	-11.08	7.55	8.12	-12.62	1.07	9.25
29	15a	-11	8.46	8.07	-12.81	8.46	8.07
30	15b	-10.54	18.87	7.72	-10.7	14.44	7.84
31	16a	-11.38	4.59	8.34	-11.69	2.68	8.57
32	16b	-10.95	17.28	7.76	-10.33	26.9	7.57
33	17a	-11.19	6.26	8.2	-11.69	2.72	8.57
34	17b	-10.78	12.52	7.9	-11.78	2.31	8.64
35	18a	-12.03	1.51	8.82	-11.51	3.68	8.43
36	18b	-11.5	3.7	8.43	-12.24	1.07	8.97
37	19a	-12.34	0.89	9.05	-13.7	0.89	10.05
38	19b	-11.91	1.85	8.73	-12.67	1.85	9.28

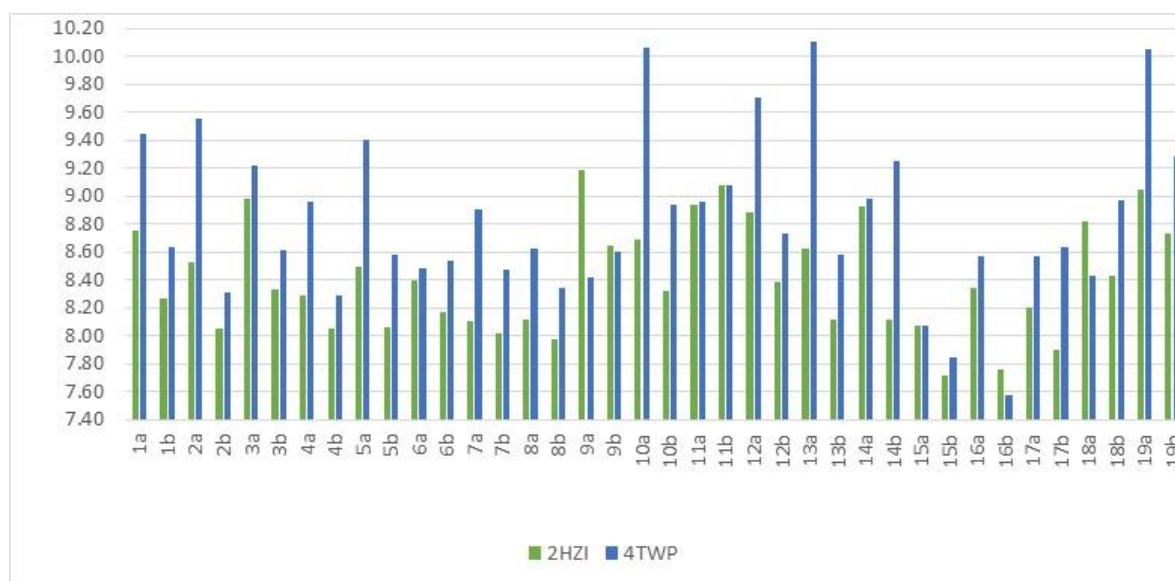


Figure 7 pKi values of the 1,5-DS-T ligands for the 2HZI and 4TWP receptors obtained from the docking studies with Autodock4

Based on a visual analysis of the docking results for each of the 1,5-DS-T ligands, we selected those that interacted with the active site of the proteins. The docking predictions indicated the 1,5-DS-T ligands to have more affinity for the 4TWP receptor (i.e., the T315I mutant) than for the 2HZI receptor. Thus, the proposed ligands may be good inhibitors for the specific ABL kinase that is resistant to imatinib.

The ligands that showed the same set of predicted interactions for the 2HZI receptor are 3a, 9a, 11a and 11b. For the 4TWP receptor, 1a, 5a, 10a and 13a displayed common interactions. The poses of the best ligands were analyzed to find the common interactions to establish the principal chemical moieties or features that contribute to the free energy and Ki results, and the results of this analysis are shown in the Figure 8. Analyzing the poses between the best 1,5-DS-T ligands for the 2HZI receptor revealed that it formed similar interactions with the halogens of three ligands, specifically with halogens attached to position 2 of the R1 substituent. The ligand with chlorine showed good predicted Ki and free energy, nevertheless the fluorine substituted with the best free energy and Ki values. As Cortes-García et al. noted in their publication of the synthesis of these novel 1,5-DS-T compounds, that including halogens in the synthesis was the highest priority in the effort to make compounds displaying a high specificity and affinity for the ABL kinase. Another interesting chemical feature was that the 1,5-DS-T ligands with the Cy substituent (R2) showed the best interactions, maybe because this moiety was interacting with a hydrophobic region in the binding site of the receptor. We chose the collection of ligands so that each one had a structural homologue as shown in Figures 8 and 9 to help relate the results to specific chemical features. At the same time, a feature that is very beneficial for our work is that the best ligands for 4TWP have almost the same pose in the binding site, as shown in Figure 9b.

Table 4. HB interactions calculated using HBAT software.

Receptor	Ligand	HB type	Donor	Acceptor	Dist. HA	Dist. XA
2HZI	9a	NH --- N	Gly249	112h	2.146	3.124
		NH --- N	Lys271	112h	2.818	3.150
		NH --- O	112h	Met318	2.129	2.956
	11b	NH --- N	Lys271	144dd	2.794	3.514
		NH --- N	Lys271	144dd	2.302	3.020
		OH --- N	Thr315	144dd	2.526	3.050
		NH --- O	144dd	Thr315	2.195	3.050
	3a	NH --- N	Gly249	96bb	1.963	2.951
		NH --- N	Lys271	96bb	2.911	3.386
		NH --- N	Lys271	96bb	2.657	2.946
		NH --- O	96bb	Met318	2.106	2.847
	11a	NH --- N	Gly249	143cc	2.948	3.165
		NH --- N	Asp 381	143cc	2.048	2.984
		NH --- N	Asp381	143cc	1.997	2.829
		NH --- N	Phe382	143cc	2.991	3.452
	4TWP	13a	NH --- N	Met316	126p	1.948
NH --- N			Met316	126p	2.380	3.113
NH --- O			Asp379	126p	2.085	2.886
NH --- O			Phe380	126p	2.959	3.824
10a		NH --- N	Met316	100a	1.974	2.970
		NH --- N	Met316	100a	2.260	3.054
1a		NH --- N	Met316	106d	2.073	3.093
		NH --- N	Met316	106d	2.118	2.997
5a		NH --- N	Met316	137w	1.911	2.931
		NH --- N	Met316	137w	2.081	2.959

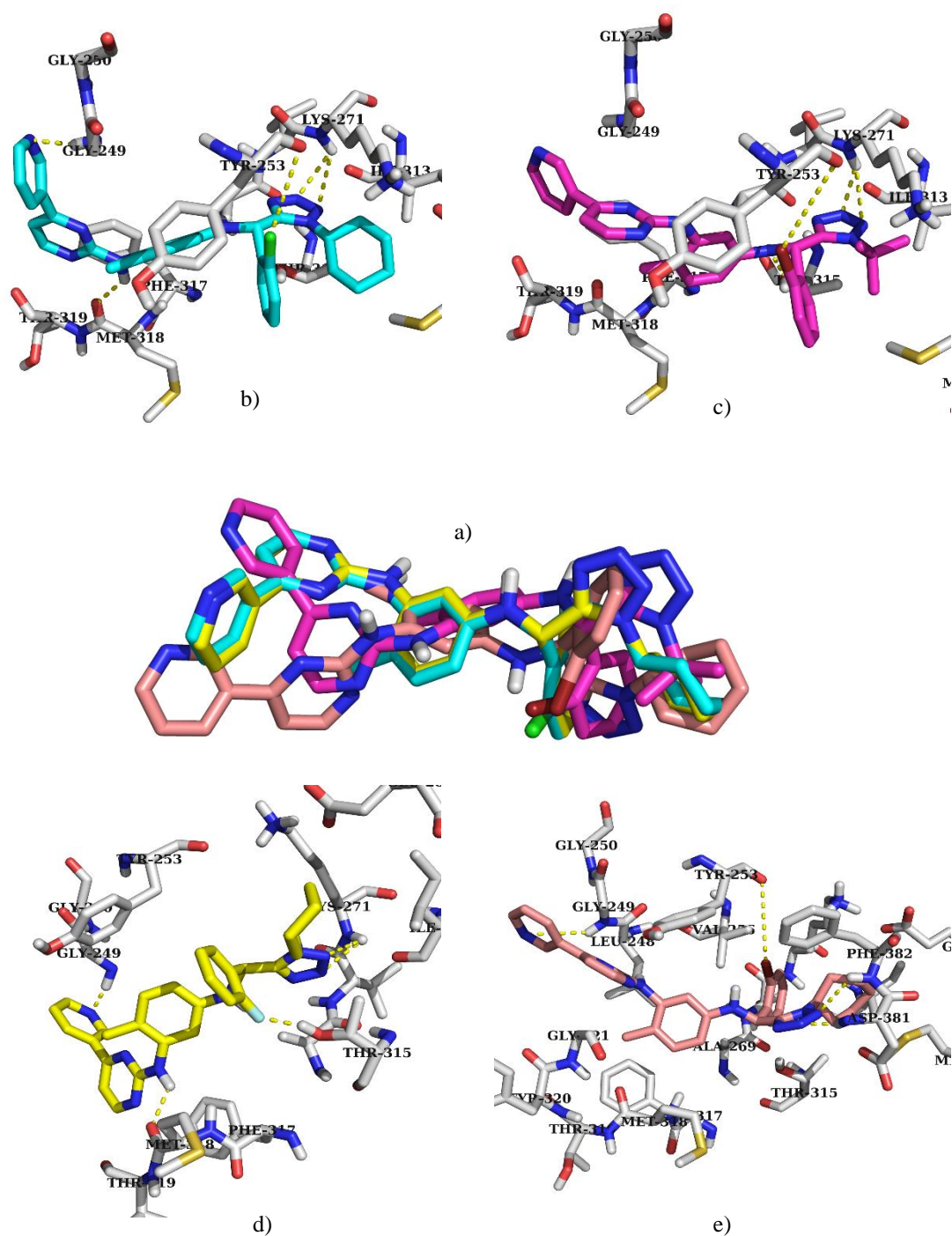


Figure 8 Alignment of the best ligands predicted for the 2HZI receptor and their interactions in the binding site. a): Alignment of the ligands 3a, 9a, 11a and 11b. Interactions of the binding site with b) 9a, c) 11b, d) 3a, and e) 11a.

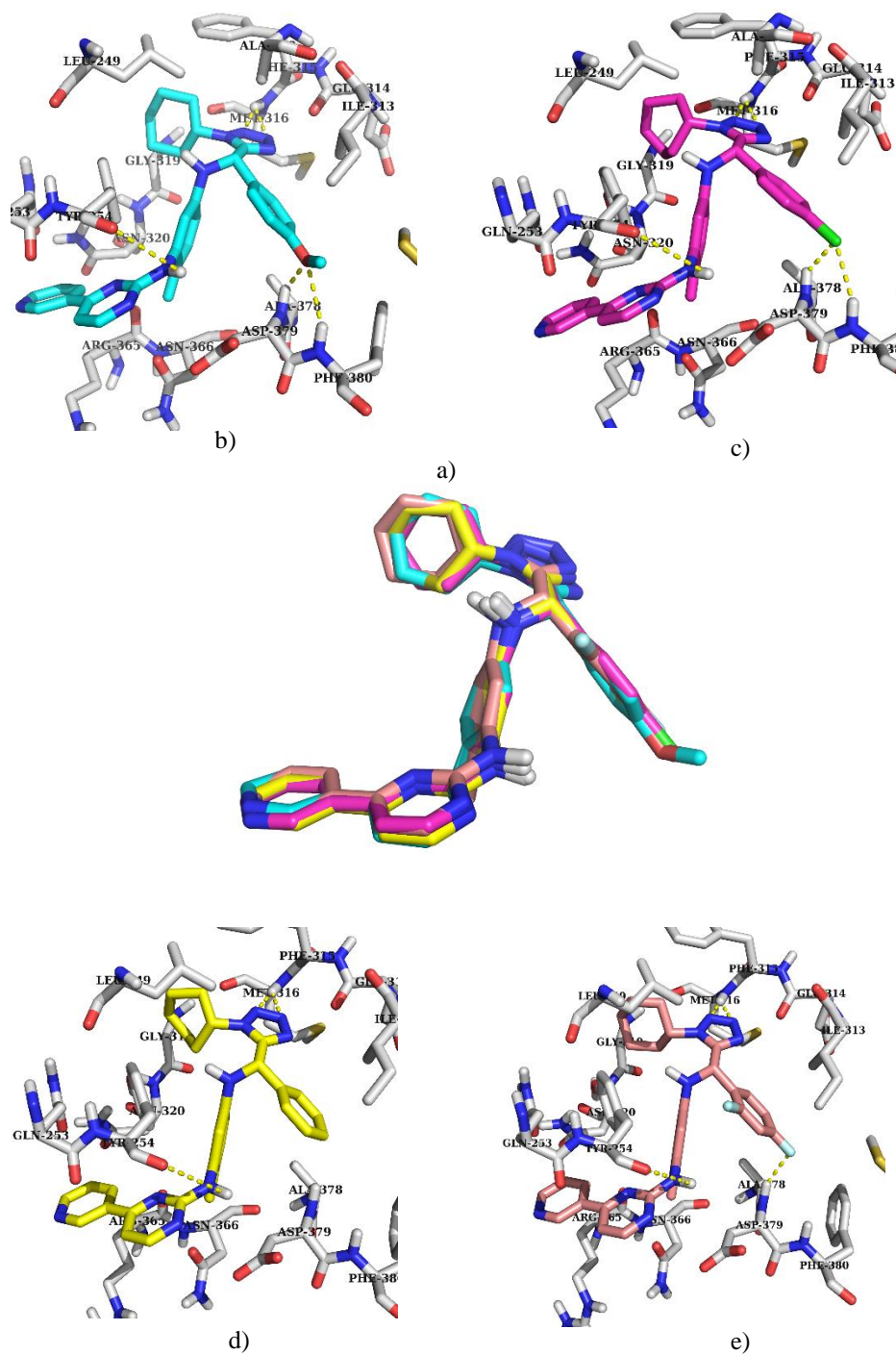


Figure 9 Alignment of the best ligands predicted for the 4TWP receptor and their interactions in the binding site. a): Alignment of the ligands 1a, 5a, 10a and 13a. Interactions of the binding site with b): 13a, c): 10a, d): 1a, and e):5a.

Table 5. Side-by-side comparison of the chemical structures of the best ligands predicted for the 4TWP receptor and the respective analogues of these ligands.

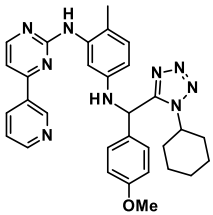
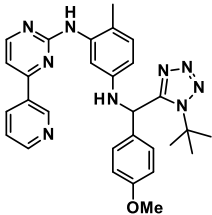
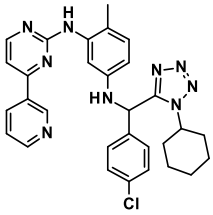
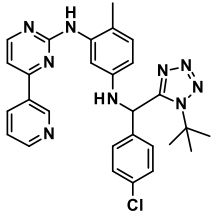
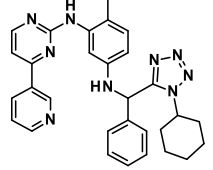
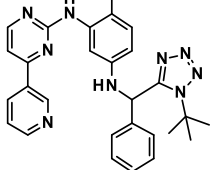
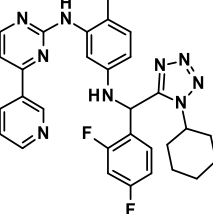
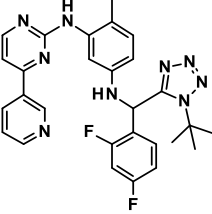
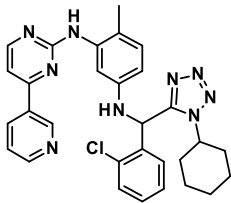
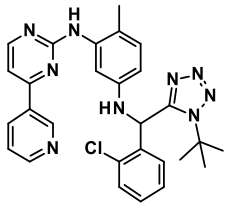
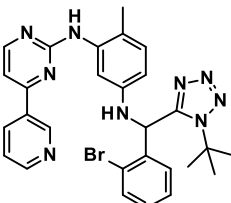
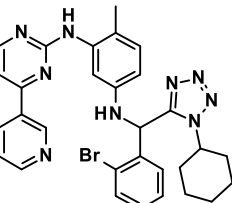
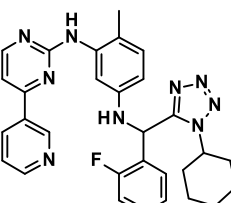
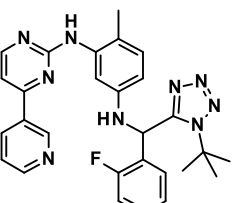
Best ligand predicted	Analogue
 <p data-bbox="264 618 703 651">13a: $\Delta G = -13.8$ kcal/mol; $K_i = 0.07$ μM</p>	 <p data-bbox="850 618 1305 651">13b: $\Delta G = -11.71$ kcal/mol; $K_i = 2.63$ μM</p>
 <p data-bbox="264 931 703 965">10a: $\Delta G = -13.73$ kcal/mol; $K_i = 0.08$ μM</p>	 <p data-bbox="850 931 1305 965">10b: $\Delta G = -12.19$ kcal/mol; $K_i = 1.15$ μM</p>
 <p data-bbox="264 1200 703 1234">1a: $\Delta G = -12.89$ kcal/mol; $K_i = 0.35$ μM</p>	 <p data-bbox="850 1200 1305 1234">1b: $\Delta G = -11.77$ kcal/mol; $K_i = 2.36$ μM</p>
 <p data-bbox="264 1514 703 1547">5a: $\Delta G = -12.82$ kcal/mol; $K_i = 0.39$ μM</p>	 <p data-bbox="850 1514 1305 1547">5b: $\Delta G = -11.7$ kcal/mol; $K_i = 2.64$ μM</p>

Table 6. Side-by-side comparison of the chemical structures of the best ligands predicted for the 2HZI receptor and the respective analogues of these ligands.

Best ligand predicted	Analogue
 <p data-bbox="261 607 707 640">9a: $\Delta G = -12.54$ kcal/mol; $K_i = 0.641$ μM</p>	 <p data-bbox="857 607 1302 640">9b: $\Delta G = -11.80$ kcal/mol; $K_i = 2.25$ μM</p>
 <p data-bbox="261 920 707 954">11b: $\Delta G = -12.54$ kcal/mol; $K_i = 0.82$ μM</p>	 <p data-bbox="857 920 1302 954">11a: $\Delta G = -12.19$ kcal/mol; $K_i = 1.16$ μM</p>
 <p data-bbox="261 1227 707 1261">3a: $\Delta G = -12.06$ kcal/mol; $K_i = 1.04$ μM</p>	 <p data-bbox="857 1227 1302 1261">3b: $\Delta G = -13.36$ kcal/mol; $K_i = 4.71$ μM</p>

Analyzing the interactions of the best 1,5-DS-T ligands for each receptor to be between the halogens attached to position 2 of the R1 in the 2HZI receptor and revealed the most common and important interactions for the 1,5-DS-T ligands with the 4TWP receptor.

From the results resumed in table 6, it is seen that the K_i values could be improved by a modification in the hydrophobic tetrazole region. In this way, docking experiments were carried out with hypothetical structures modified in this region, using the same protocol that was used for the 38 1,5-DS-T and as a receptor PDB code 2HZI. The chemical structures and their docking results are presented at the table 7. It is noteworthy that results of the ligand 9a-6 that containing the adamantly moiety, resulted with a free energy of -12.48 and a K_i of 0.705 nM (0.000705 μM) which has the lower K_i values.

Table 7. Docking results derived from 9a 1,5-DS-T ligand, where we have proposed a chemical modification in R2 (figure 3.) that improves the predicted affinity toward 2HZI crystallographic structure. Note that the K_i values obtained are predicted in a nM concentration.

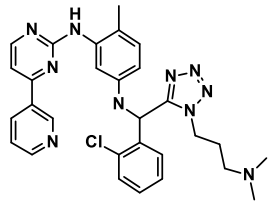
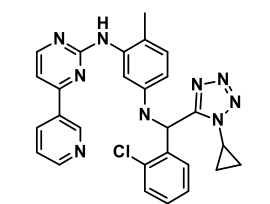
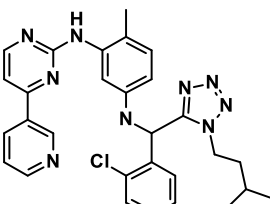
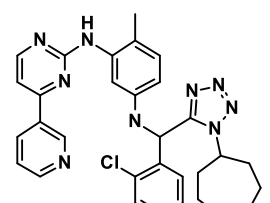
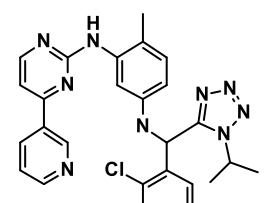
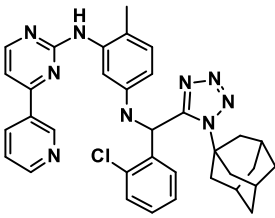
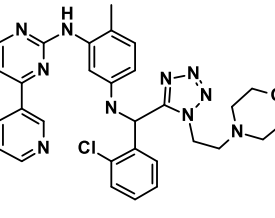
Chemical structure	Predicted ΔG (kcal/mol)	K_i (nM)
 <p>9a-1</p>	-11.94	1.78
 <p>9a-2</p>	-11.41	4.30
 <p>9a-3</p>	-11.60	3.12
 <p>9a-4</p>	-12.35	0.87
 <p>9a-5</p>	-11.20	6.2

Table 7. Docking results derived from 112h 1,5-DS-T ligand, where we have proposed a chemical modification in R2 (figure 3.) that improves the predicted affinity toward 2HZI crystallographic structure. Note that the K_i values obtained are predicted in a nM concentration. (Continuation)...

Chemical structure	Predicted ΔG (kcal/mol)	K_i (nM)
 <p style="text-align: center;">9a-6</p>	-12.48	0.705
 <p style="text-align: center;">9a-7</p>	-12.58	1.04

4. Conclusions

The halogen interaction is important for the binding mode of these 1,5-DS-T ligands [34]. Two possible interactions would arise from hydrogen bonding or sigma hole interactions. To demonstrate this, an appropriate scoring function as Autodock VinaXB [35], or QM/MM combined with GMBSA [36], could be used.

5. Conflict of interest

The authors declare no conflict of interest.

6. Acknowledgments

We thank to CONACyT for the fellowship 305150, and to the Universidad Michoacana support from CIC-UMSNH (2.18).

References

1. Ben-Neriah, Y.; Q. Daley, G.; Mes-Masson, A. M.; N. Witte, O.; Baltimore, D. The chronic myelogenous leukemia-specific P210 protein is the product of the bcr/abl hybrid gene. *Science*, **1986**, *233*, 212–214, DOI: 10.1126/science.3460176
2. Von Bubnoff, N.; Duyster, J. Chronic myelogenous leukemia: treatment and monitoring. *Dtsch Arztebl Int*, **2010**, *107*, 114–21, DOI: 10.3238/arztebl.2010.0114
3. Colicelli, J. ABL Tyrosine Kinases: Evolution of Function, Regulation, and Specificity. *Science Signaling*, **2011**, *3*, 139, DOI: 10.1126/scisignal.3139re6.
4. T. Abelson, H.; S. Rabstein, L. Lymphosarcoma: Virus-induced Thymic-independent Disease in Mice. *Cancer Research*, **1970**, *30*, 2213–2222, DOI: Published August 1970.

5. Kumar, H.; Raj, U.; Gupta, S.; Tripathi, R.; Kumar Varadwaj, P. Systemic Review on Chronic Myeloid Leukemia: Therapeutic Targets, Pathways and Inhibitors. *J Nucl Med Radiat Ther*, **2015**, *6*, 1-7, DOI: 10.4172/2155-9619.1000257
6. Baccarani, M.; Deininger, M.W.; Rosti, G.; Hochhaus, A.; Soverini, S.; Apperley, J.F.; Cervantes, F.; Clark, R. E.; Cortes, J. E.; Guilhot, F.; Hjorth-Hansen, H.; Hughes, T. P.; Kantarjian, H. M.; Kim, D. W.; Larson, R. A.; Lipton, J. H.; Mahon, F. X.; Martinelli, G.; Mayer, J.; Muller, M. C.; Niederwieser, D.; Pane, F.; Radich, J. P.; Rousselot, P.; Saglio, G.; Sabele, S.; Schiffer, C.; Silver, R.; Simonsson, B.; Steegmann, J. L.; Goldman, J. M.; Hehlmann, R. European LeukemiaNet recommendations for the management of chronic myeloid leukemia: 2013. *Blood*, **2013**, *122*, 872–884, DOI: 10.1182/blood-2013-05-501569.
7. Kantarjian, H.; Sawyers, C.; Hochhaus, A.; Guilhot, F.; Schiffer, C.; Gambacorti-Passerini, C.; Niederwieser, D.; Resta, D.; Capdeville, R.; Zoellner, U.; Talpaz, M.; Druker, B. Hematologic and cytogenetic responses to imatinib mesylate in chronic myelogenous leukemia. *N Engl J Med* **2002**, *346*, 9, 645–652, DOI: 10.1056/NEJMoa011573.
8. Capdeville, R.; Buchdunger, E.; Zimmermann, J.; Matter, A. Glivec (STI571, imatinib), a rationally developed, targeted anticancer drug. *Nat Rev Drug Discov* **2002**, *1*, 403–502, DOI: 10.1038/nrd839.
9. Desogus, A.; Schenone, S.; Brullo, C.; Tintori, C.; Musumeci, F. Bcr-Abl tyrosine kinase inhibitors: a patent review. *Expert Opinion Ther. Patents*, **2015**, *25*, 1–16, DOI: 10.1517/13543776.2015.1012155.
10. O'Hare, T.; Shakespeare, W. C.; Zhu, X.; Eide, C. A.; Rivera, V. M.; Wang, F.; Adrian, L. T.; Zhou, T.; Huang, W.-S.; Xu, O.; Metcalf, C. A.; Tyner, J. W.; Loriaux, M. M.; Corbin, A. M.; Wardwell, S.; Ning, Y.; Keats, J. A.; Wang, Y.; Sundaramoorthi, R.; Thomas, M.; Zhou, D.; Snodgrass, J.; Commodore, L.; Sawyer, T. K.; Dalgarno, D. C.; Deininger, M. W. N.; Druker, B. J.; Clackson, T. AP24534, a pan-BCR-ABL inhibitor for chronic myeloid leukemia, potently inhibits the T315I mutant and overcomes mutation-based resistance. *Cancer Cell*, **2009**, *16*, 5, 401–412, DOI: 10.1016/j.ccr.2009.09.028.
11. Zhou, T.; Parillon, L.; Li, F.; Wang, Y.; Keats, J.; Lamore, S.; Xu, O.; Shakespeare, W.; Dalgarno, D.; Zhu, X. Crystal structure of the T315I mutant of Abl kinase. *Chem Biol Drug Des*, **2007**, *70*, 171–181, DOI: 10.1111/j.1747-0285.2007.00556.x.
12. Pemovska, T.; Johnson, E.; Kontro, M.; Repasky, G. A.; Chen, J.; Wells, P.; Cronin, C. N.; McTigue, M.; Kallioniemi, O.; Porkka, K.; Murray, B. W.; Wennerberg, K. Axitinib effectively inhibits BCR-ABL1 (T315I) with a distinct binding conformation. *Nature*, **2015**, *5*, 102–105, DOI: 10.1038/nature14119.
13. Cortes-García, C. J.; Jácome, A.; Rentería, A.; Gámez, R. Synthesis of 1,5-disubstituted tetrazoles containing a fragment of the anticancer drug imatinib via a microwave-assisted Ugi-azide reaction. *Monat Fur Chem*, **2016**, *147*, 1277–1290, DOI: <https://doi.org/10.1007/s0070>.
14. Huang, N.; Schoichet, B. K.; Irwing, J. J. Benchmarking Sets for Molecular Docking. *J Med Chem*, **2006**, *49*, 6789–6801, DOI: 10.1021/jm0608356.
15. Swain, M. chemicalize.org. *J Chem Inf Model*, **2012**, *52*, 613–615, DOI: 10.1021/ci300046g.
16. Casewit, C. J.; Colwell, K. S.; Rappé, A. K. Application of a Universal Force Field to Organic Molecules. *J Am Chem Soc.* **1992**, *114*, 10035–10046, DOI: 10.1021/ja00051a041.
17. Gaussian 09, Revision E.01, Frisch M. J.; Trucks, G. W.; Schlegel, H. B.; Scuseria, G. E.; Robb, M. A.; Cheeseman, J. R.; Scalmani, G.; Barone, V.; Mennucci, B.; Petersson, G. A.; Nakatsuji, H.; Caricato, M.; Li, X.; Hratchian, H. P.; Izmaylov, A. F.; Bloino, J.; Zheng, G.; J. L.; Hada, M.; Ehara, Toyota, M. K.; R.; Fukuda, J.; Hasegawa, M.; Ishida, T.; Nakajima, Y.; Honda, O.; Kitao, H.; Nakai, T.; Vreven, J. A.; Montgomery, Jr., J. E.; Peralta, F.; Ogliaro, M.; Bearpark, J. J.; Heyd, E.; Brothers, K. N.; Kudin, V. N.; Staroverov, R.; Kobayashi, J.; Normand, K.; Raghavachari, A.; Rendell, J. C.; Burant, S. S.; Iyengar, J.; Tomasi, M.; Cossi, N.; Rega, J. M.; Millam, M.; Klene, J. E.; Knox, J. B.; Cross, V.; Bakken, C.; Adamo, J.; Jaramillo, R.; Gomperts, R. E.; Stratmann, O.; Yazyev, A. J.; Austin, R.; Cammi, C.; Pomelli, J. W.; Ochterski, R. L.; Martin, K.; Morokuma, V. G.; Zakrzewski, G. A.; Voth, P.; Salvador, J. J.; Dannenberg, S.; Dapprich, A. D.; Daniels, Ö.; Farkas, J. B.; Foresman, J. V.; Ortiz, J.; Cioslowski, and D. J. Fox, Gaussian, Inc., Wallingford CT, **2009**
18. Sanner, M. F. Python: a programming language for software integration and development, *J Mol Graph Model*, **1999**, *17*, 57–61, DOI: 10.1016/S1093-3263(99)99999-0.
19. Forli, S.; Huey, R.; Pique, M. E.; Sanner, M. F.; Goodsell, D. S.; Olson, A. J.; Computational protein–ligand docking and virtual drug screening with the AutoDock suite. *Nature protocols*, **2016**, *11*, 905–919, DOI: 10.1038/nprot.2016.051.

20. Rose, P. W.; Prlic, A.; Bi, C.; Bluhm, W. F.; Christie, C. H.; Dutta, S.; Green, R. K.; Goodsell, D. S.; Westbrook, J. D.; Wool, J.; Young, J.; Zardecki, C.; Berman, H. M.; Bourne, P. H.; Burley, S. K. The RCSB Protein Data Bank: views of structural biology for basic and applied research and education. *Nucl Acids Res*, **2015**, *43*, 345–356, DOI: 10.1093/nar/gku1214.
21. Cowan-Jacob, S. W.; Fendrich, G.; Floersheimer, A.; Furet, P.; Liebetanz, J.; Rummel, G.; Rheinberger, P.; Centeleghe, M.; Fabbro, D.; Manley, P. W. Structural biology contributions to the discovery of drugs to treat chronic myelogenous leukaemia. *Biological Crystallography* **2007**, *63*, 80–93, DOI: 10.1107/S0907444906047287.
22. Kaplan W.; Littlejohn, T. G. Swiss-PDB Viewer (Deep View). *Briefings in Bioinformatics*, **2001**, *2*, 195-197, DOI: <https://doi.org/10.1093/bib/2.2.195>.
23. Morris, G. M.; Goodsell, D. S.; Halliday, R. S.; Huey, R.; Hart, W. E.; Belew, R. K.; Olson, A. J. Automated docking using a Lamarckian genetic algorithm and an empirical binding free energy function. *J Comp Chem*, **1998**, *19*, 1639-1662, DOI: 10.1002/(SICI)1096-987X(19981115)19:14<1639::AID-JCC10>3.0.CO;2-B.
24. Gallardo, S.; Ocampo, A. L.; Contreras, C. A.; Chacón, L. Synthesis and Docking Studies of the Novel N-(2,2-Di(1H-pyrrol-2-yl)ethyl)adamantane-1-carboxamide, a Potential 11 β -HSD1 Inhibitor. *Journal of Chemistry Hindawi*, **2014**, 1-5, DOI:10.1155/2014/294246
25. Triballeau, N.; Acher, F.; Brabet, I.; Pin, J. P.; Bertrand, H. O. Virtual Screening Workflow Development Guided by the “Receiver Operating Characteristic” Curve Approach. Application to High-Throughput Docking on Metabotropic Glutamate Receptor Subtype 4. *J Med Chem*, **2005**, *48*, 2534-2547, DOI: 10.1021/jm049092j.
26. Tiwari, A.; Panigrahi, S. K. HBAT: A Complete Package for Analysing Strong and Weak Hydrogen Bonds in Macromolecular Crystal Structures. *In Silico Biology*, **2007**; *6*; 651–661, DOI: content.iospress.com/articles/in-silico-biology/isb00337
27. Lavecchia, A. Machine-learning approaches in drug discovery: Methods and applications. *Drug Discov Today*, **2014**, *20*, 318-331, DOI:10.1016/j.drudis.2014.10.012
28. Ghaaliq, A.; McCluskey, A. Clinical tests: sensitivity and specificity. *Continuing Education in Anaesthesia, Critical Care & Pain*. **2008**; *8*; 221–223, DOI: 10.1093/bjaceaccp/mkn041
29. Auffinger, P.; Hays, F. A.; Westhof, E.; Shing Ho P. Halogen bonds in biological molecules. *Proc Natl Acad Sci USA*, **2004**; *101*, 16789-16794, DOI: 10.1073/pnas.0407607101.
30. Regier, A.; Khuu, P.; Oishi, K.; Shing Ho P. Halogen bonds as orthogonal molecular interactions to hydrogen bonds. *Nat Chem*, **2009**; *1*; 74–79, DOI: 10.1038/nchem.112.
31. Lu, X.; Wang, Y.; Zhu, W. Nonbonding interactions of organic halogens in biological systems: implications for drug discovery and biomolecular design. *Phys Chem Chem Phys*, **2010**, *12*, 4543–04551, DOI: 10.1039/B926326H.
32. Sirimulla, S.; Bailey, J. B.; Vegesna, R.; Narayan, M. Halogen Interactions in Protein–Ligand Complexes: Implications of Halogen Bonding for Rational Drug Design. *J Chem Inf Model*, **2013**, *53*, 2781- 2791, DOI: 10.1021/ci400257k.
33. Kortagere, S.; Ekins, S.; Welsh, W. J. Halogenated ligands and their interactions with amino acids: implications for structure-activity and structure-toxicity relationships. *J Mol Graph Model*, **2008**, *27*, 170–177, DOI: <https://doi.org/10.1016/j.jmgm.2008.04.001>.
34. Cavallo, G.; Metrangolo, P.; Milani, R.; Pilati, T.; Priimagi, A.; Resnati, G.; Terraneo, G. The Halogen Bond. *Chem Rev*, **2016**, *116*, 2478-2601, DOI 10.1021/acs.chemrev.5b00484.
35. Koebel, M. R.; Schmadeke, G.; Posner, R. G.; Sirimulla, S. AutoDock VinaXB: implementation of XBSF, new empirical halogen bond scoring function, into AutoDock Vina. *Journal of Cheminformatics*, **2016**, 8-27, DOI: <https://doi.org/10.1186/s13321-016-0139-1>.
36. Kurczab, R. The evaluation of QM/MM-driven molecular docking combined with MM/GBSA calculations as a halogen-bond scoring strategy. *Acta Crystallographica*, **2017**, *B73*, 188-194, DOI: 10.1107/S205252061700138X.

